A Photoreactive G-quadruplex Ligand Triggered by Green Light.

Matteo Nadai,‡ Filippo Doria,‡ Luca Germani, Sara N. Richter,* Mauro Freccero*.

[1] *Department of Chemistry, University of Pavia, V.le Taramelli 10, 27100 Pavia, Italy*

[2] *Department of Molecular Medicine, University of Padua, via Gabelli 63, 35121, Padua, Italy.*

Supporting Information Placeholder

ABSTRACT: A Photo-reactive molecular dye targeting the G-quadruplex structure (G4) of the human telomeric sequence (Tel22), and several mutated analogues, has been triggered by green light (λ_{abs}=525 nm). Gel electrophoresis data showed a highly selective covalent modification of G4 *vs* scrambled single-stranded and double-stranded DNA, with alkylation efficiency up to 64%. Phenoxyl radical has been generated by photo-induced electron transfer as reactive intermediate targeting loop Ts, detecting it by laser flash photolysis. These insights may suggests a non-invasive tool for G4 tagging and *pull-down* cellular applications.

G-quadruplexes (G4s) are four stranded nucleic acid secondary structures, which may form in G-rich sequences.[1] The existence of G4s has been described in several genomic regions, such as in gene promoters[2] and telomere.[3] G4 formation has been visualized in human cell where they become significant during cellular replication.[4] The most recent investigations on this target aim at defining the G4 potential role as regulatory elements and/or therapeutic targets. In this context, a large variety of small molecules acting as reversible G4 ligands have been exploited as flexible G4 interacting tools in biological studies. Nevertheless, the targeting has seldom been achieved successfully through covalent interactions between the ligands and the target. In the sporadic reported examples, such a G4 targeting strategy has been achieved conjugating the recognition element to chemically reactive moieties such as quinone methides,[5] epoxides,[6] platinum complexes[7] and Chlorambucil.[8] In order to minimize off-target effects in a cellular environment two key issues have to be addressed: (i) selective recognition of the G4 and (ii) activation of the chemical reactivity on demand by external stimuli (chemical reduction, oxidation or irradiation).[9] In this context, the intrinsic photochemistry of G4 DNA has been investigated. The photoinduced hydrogen abstraction reactions of iodouracil substituted telomeric DNA has been reported.[10] Cech and coworkers reported the first formation of crosslinks upon 254 nm irradiation of the folded form of the d(T4G-4)4, and d(T2G-4)4 telomeric sequences as evidence for a G-4 structure.[11] Recently, it has been suggested that the detection of thymine dimers, resulting from the irradiation of the folded human telomeric sequence d[AG3(T2AG3)3] (Tel22) with UVB light (280–320 nm), may be used as diagnostic tool to establish the presence of G-4 structures in vivo.[12] Even more recently, both human telomeric G4 and the oncogene promoter *c-myc* have been covalently targeted by a bisquinolinium pyridodicarboxamide ligand tethered to benzophenone as photo-cross-linking moiety, by UVA irradiation (330–365 nm).[13] Both the intramolecular and the ligand-mediated photo-reactivity on G4 have certainly been propelled by the potential and useful applications of a G4 tagging and *pull-down* process, by covalent modifications.[14] Nevertheless, it has to be kept in mind that G4 photo-induced reactions using UV irradiation will surely hamper the potential applications *in cellulo*, due to the competitive ds (double-stranded) DNA thymine-thymine cross-linking.[15] Such a major drawback can be erased using a photo-induced reaction between a colored photo-reactive ligand and the G4 substrate. To our knowledge, the opportunity to use visible light (λ>400nm) to trigger an efficient and selective covalent damage on G4 has not yet been described. This is surprising, as a large variety of G4 ligands are colored dyes, which fluorescence is quenched upon binding. Among them, naphthalene diimides (NDIs), which have been extensively investigated by us and others, exhibit unique and tunable photo-physical and redox properties,[16] which deserve to be exploited for the purpose.[17]

Figure 1. NDI dyes absorbing green light. Absorption of **2** ($3x10^{-5}$M), in water solution (black line) and in the presence of Tel22 ($4x10^{-6}$M → $6x10^{-5}$M, red and orange lines).

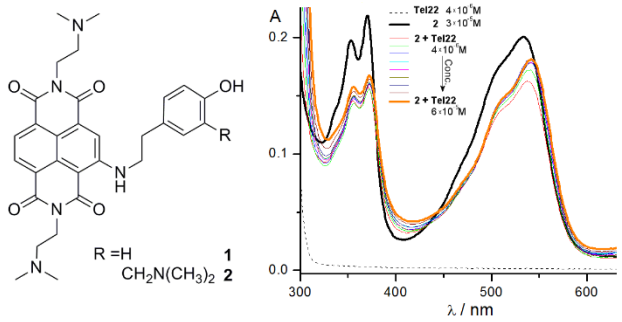

The synthesis, binding and photophysical properties of tri-substituted NDI dyes (λ_{max} 525 nm) conjugated to phenol moieties (**1** and **2**, Figure 1) in the presence of Tel22 have been previously investigated, highlighting a selective and effective reversible targeting mode.[5b] To evaluate the photo-reactivity of **1** and **2**, we investigated their photo-physical and photo-chemical behavior in both neat acetonitrile (ACN) and in water solution, under neutral and slightly acidic conditions (phosphate buffered, pH 7 and 5) by laser flash photolysis (LFP) using a Nd:YAG laser. Upon green light (532 nm) laser excitation, a full spectra assigned to the triplet excited state of **2** was recorded in the range of 380−750 nm (λ_{max} 430 nm), in both ACN (using **2** as tri-hydrochloride, **2**·3HCl, Figure S1) and under aqueous acid conditions (pH 5.0, phosphate buffered, Figure S2). The pKa values of **2**, measured by a potentiometric titration (6.8, 7.7 and 9.2, Figure S3), suggested a partially un-protonated -CH2NMe2 moiety, under neutral conditions,

and the occurrence of a very fast intramolecular electron transfer (eT), which was too quick to be detected by our LFP equipment. Therefore, we decided to investigate a slower bimolecular photo-induced eT (PeT) process between the model NDI **3** and both the phenol **4** and the Mannich base **5**, respectively (Chart 1, Supp. Inf.).

Chart 1. NDI-3 and quenching phenols 4 and 5, investigated as a bimolecular photoreaction model.

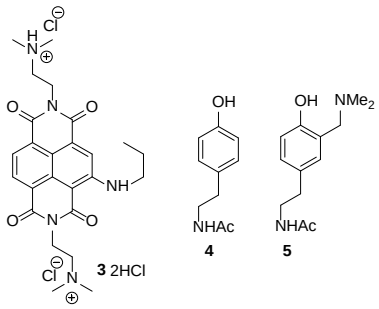

In the presence of the quencher **5**, the triplet excited state of **3** followed a mono-exponential decay, with k1 = $kq_{obs}C$, where kq_{obs} was the observed quenching rate constant (kq_{obs}=1.9±0.1 $10^{10}M^{-1}s^{-1}$ and 4.8±0.1 $10^{9}M^{-1}s^{-1}$ in ACN and buffer at pH 5.5, respectively), which was extracted from Stern−Volmer plots (Figure S4a-b) and C the concentration of the quencher. Contrary, the phenol **4** was a poorer quencher with a kq_{obs} 3.9 $10^{8}M^{-1}s^{-1}$ in ACN (Figure S4c). This was not surprising as Mannich bases with strong intramolecular H-bonding, such as **5**, exhibit a lower oxidation potential than the phenol analogues.[18] The kq_{obs} values suggest a barrierless PeT from Mannich base to the **3**-triplet excited state (^{3}**3***, λ_{max} at 430 nm, Figure 2a, blue line) only, generating the radical anion $\mathbf{3}^{\bullet-}$ (λ_{max} at 470 and 490 nm),[19] and the radical cation $\mathbf{5}^{\bullet+}$ (Figure 2a red line). For an unambiguous assignment of both radical ions, $\mathbf{3}^{\bullet-}$ was generated in an independent way, in the absence of the radical cation counterpart, flashing **3** in the presence of 4-methoxybenzyltrimethylsilane (Figure 2b, red line). In fact, the radical cation of the latter underwent a fast unimolecular fragmentation yielding a benzyl radical and a $Me3Si^{+}$ cation, both undetectable by LFP.[20] $\mathbf{5}^{\bullet+}$ absorption spectra became clearly detectable generating the transient species in the presence of a radical anion scavenger such as O_2, which quenches the radical anion $\mathbf{3}^{\bullet-}$ (Figure 2c, red line). The radical cation $\mathbf{5}^{\bullet+}$ exhibits an UV-visible absorption characteristic of a phenoxyl radical, centered at 410 nm, with a broad and weak absorption at 600 nm.[18b, 21] Therefore, our LFP data on the bimolecular model suggest that the NDI **2** should be able to generate phenoxyl radical upon green light irradiation (532 nm).

Figure 2. Irradiation @ 532 nm of **3** (ACN solution, $3.5x10^{-4}$ M) in the presence of: a) **5** ($2.4x10^{-4}$M) under O_2 free conditions, spectra recorded from the laser shot to 34 µs, b) 4-methoxybenzyltrimethylsilane ($8.5x10^{-2}$M), O_2 free, c) **5** ($2.4x10^{-4}$M) and air, spectra recorded from 0.84 to 2.08 µs, after the laser shot.

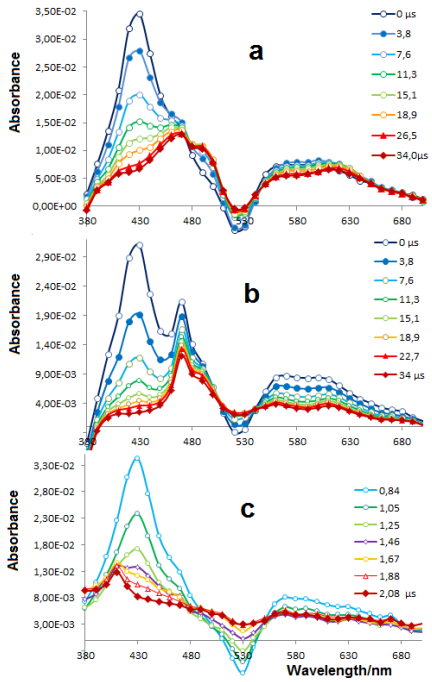

Following the notion that phenoxyl radicals react as C-radicals at the *ortho*-position with thymine and thymidine,[22] we investigated the ability of NDIs to deliver reactive phenoxyl radicals, generated by intramolecular PeT, onto the thymines of the Tel22 loops. The photoreactivity of **2** in the presence of the G4 folded Tel22, scrambled (scr, same base composition in a sequence unable to fold into G4) ss and ds Tel22 was initially assessed. Increasing amounts of compound **2** (12 nM – 50 µM) were irradiated with the folded or scr ^{32}P-labelled Tel22 templates (0.25 µM), at 20°C for 24 h, using visible light (1 lamp, 15 W, 400 nm<λ<650 nm). Identical samples were incubated in the dark. The reaction samples were analysed by denaturing polyacrylamide gel electrophoresis (PAGE). A concentration dependent lower mobility band was observed in the presence of the G-4 folded Tel22, from 50 nM to 12.5 µM (0.2:1 to 50:1 **2**/Tel22 ratio). The adduct yield was 64% at 12.5 µM (Figure 3). To our knowledge this is the highest covalent adduct efficiency ever achieved for a telomeric G4 targeting. In contrast, the same band was barely detectable in the scrambled ss Tel22 substrate and absent in the scrambled ds oligonucleotide, even when treated with 200:1 **2**/Tel22 ratio (Figure 3). These data indicate a remarkable selective interaction of the G4 structure over unstructured or double helix DNA by **2**. Irradiation of **1** with the G4 folded Tel22 under identical conditions produced at the highest concentrations only a faint band with similar gel mobility (Figure S5). The lack of reactivity of **1** is consistent with LFP data, as the phenol moiety is more difficult to be oxidised by the triplet-excited state of the NDI core than its Mannich base analogue.

Figure 3. PAGE under denaturing conditions of increasing amounts of **2** in the presence of the G4 folded Tel22, scr, ss and ds Tel22, upon visible light irradiation. Control samples were either irradiated with visible light in the absence of **2** or incubated in the dark in the presence of **2** at 50µM.

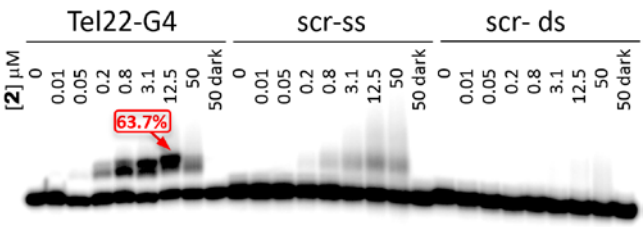

Matrix-assisted laser desorption/ionization time-of-flight (MALDI-TOF) mass spectrometry of a typical reaction mixtures using a 12.5 μM concentration of **2** displayed abundant signal corresponding to unreactive Tel22 (6966 Da), together with an additional signal detected for a species with 7568 Da (Figure S6), in agreement with a M+1 adduct of Tel22 construct with **2.** The possible reversible character of the **2**-Tel22 adduct was evaluated as a function of temperature and salt concentration. The adduct was stable after 10 min incubation at 95°C (Figure S7a) and in a 0.5 M KCl solution (Figure S7b). Therefore, the bands with lower mobility were attributed to a covalent modified Tel22 as the photoadducts provide additional mass and positive charges. In order to directly identify the specific base involved in the photoreaction, we constructed three telomere sequences Tel22-C*n* (*n*= 1, 2, 3), in which the first (n=1), second (n=2) Ts or third base A (n=3) in the three TTA loops were simultaneously replaced with Cs. A fourth telomere sequences Tel22-T3, in which the As of the loops, were replaced with Ts was investigated as well (Figure 4).

Figure 4. PAGE (denaturing conditions) of Tel22 and mutant Tel22 oligonucleotides in the presence of **2** and visible light.

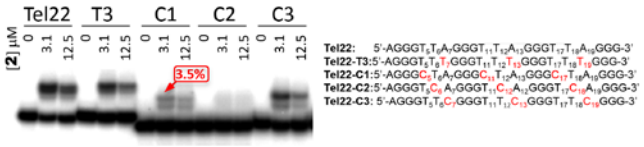

Mutant Tel22-T3 and Tel22-C3 generated gel bands upon irradiation, with similar mobility and only slightly lower efficiency to that achieved with the unmodified Tel22. Therefore, loop adenines appear not to be the main target sites. On the contrary, the efficiency of the covalent adduct generation was strongly affected by mutations replacing Ts with Cs. In fact, Tel22-C2 was fully unreactive, as no covalent adduct was detected by irradiation in the presence of **2** (Figure 4). Likewise, Tel22-C1 was alkylated to a very low extent (3.5% yield). The similar dichroic behaviour of the four modified oligonucleotides in the presence of NDI **2** suggests that the striking selective photo-reactivity between Tel22 and Tel22-C2 could not be ascribed to different topologies (Figure 5). Therefore, such a remarkable selectivity is likely to be caused by the different base composition of the loops, in particular, by the presence of accessible Ts in the middle of the loop, such as T6, T12 and T18. The evaluation of the alkylation selectivity on three additional mutant Tel22, namely C2a, C2b and C3c (see Figure 6 for composition and Figure S8 for CD spectra) suggested T12 and T6 as the most reactive Ts of the sequence. In fact, their replacement caused a detectable reduction of the alkylation efficiency.

Figure 5. CD spectra of Tel22, and modified oligoes (4 μM) in the presence of **2** (16 μM), in Tris-buffer, 50 mM KCl, pH 7.

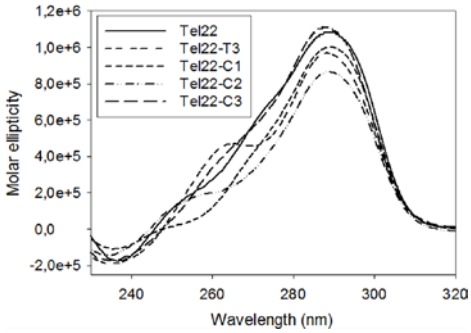

Figure 6. PAGE (denaturing conditions) of Tel22-C2 and single nucleotide mutants in the presence of **2** and visible light.

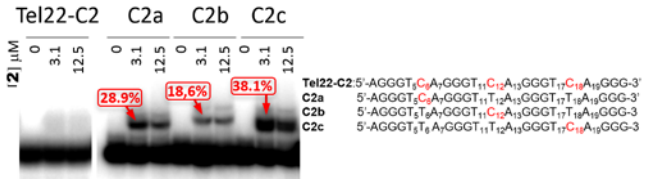

To further characterize the sites of alkylation by **2** on Tel22, the purified adduct along with the untreated Tel22 was subjected to enzymatic digestions by Exonuclease I (ExoI) and S1 Nuclease (S1). S1 cuts oligonucleotides in ss regions, therefore the alkylated oligonucleotide will be cut at ss bases which were not alkylated. First, the sites of S1 cleavage on the non-alkylated Tel22 were assessed by comparison with the Maxam and Gilbert marker. Next, S1-induced cleavage sites on the alkylated Tel22 were assessed by comparison with the non-alkylated Tel22, considering that alkylation makes all bands run slower in the gel. As shown in Fig. 7A, in the non-alkylated Tel22, main sites of S1 cleavage were T18/A19 (symbol ¤, S1, N lane) and T12/A13 (symbol §, S1, N lane). Cleavage at the T5-A7 loop could not be observed as discrete bands at the single nucleotides, but as a major band corresponding to G4 suggesting the presence of extensive cleavage at the T5-A7 loop. In the alkylated Tel22 (S1, A lane), T18/A19 and A13 cleavage sites were present, while remarkable less cleavage was observed at T12. In addition, no cleavage was obtained at the T5-A7 loop probably due to the presence of a major alkylation site at this level. The S1 cleavage pattern served also to evaluate the upward shifting of the bands in the alkylated sample with respect to the non-alkylated bands (Fig. 7B) along the whole sample lane. Thus we were able to calculate the position of cleavage obtained with ExoI in the alkylated Tel22. ExoI cuts oligonucleotides in the 3' to 5' direction and the principle of this assay is that ExoI cleavage will be hindered at alkylation sites which will thus be observed as discrete bands. Pausing sites in the alkylated Tel22 were observed at positions T6 (symbol ^) and T12 (symbol @), which are consistent with results by CD analysis. An additional minor site was found at G14/G15 (symbol #), which could not be detected by CD mutation analysis, due to the impossibility to create mutants at Gs still retaining the G-quadruplex conformation. G involvement may depend on initial reaction at Ts.

Figure 7. a) Sequencing gel of the purified non-alkylated (N) and alkylated (A) Tel22 samples subjected to ExoI and S1 digestion. M, marker lanes by the Maxam and Gilbert reaction to visualize Gs and As. b) Linear correlation between S1 digested sites in the alkylated and non-alkylated samples (solid line and black circles); the dashed line and white circles were extrapolated to obtain the cleavage position of the ExoI sites of the alkylated sample.

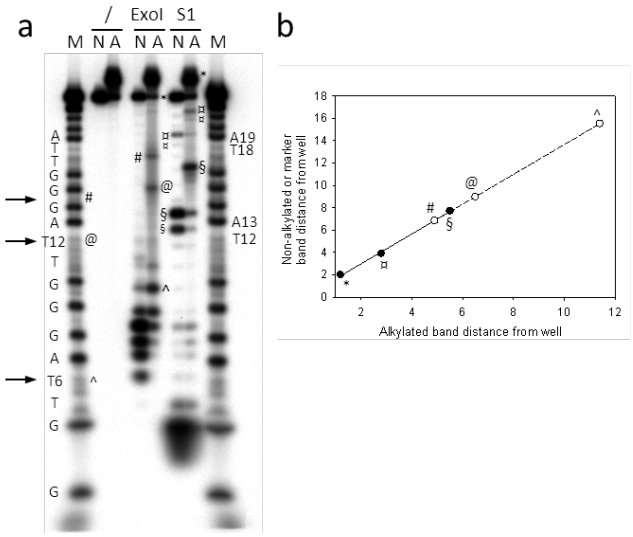

Our data consistently suggest a selective covalent targeting of the loop Ts in the wild type Tel22 and mutated Tel22 containing Ts in the loop. The observed reactivity has to be ascribed to a phenoxyl radical generated by intramolecular PeT occurring in the **2**-Tel22 complex. To our knowledge this is the first example of a very selective and efficient G4 covalent modification activated by green light. Taking into account that 532 nm is the first harmonic of commercial solid state lasers, the photo-reactivity of **2** towards G4 structures opens up a great opportunity for efficient G4 covalent targeting by carbon radicals, for tagging and *pull-down* applications.

ASSOCIATED CONTENT

Supporting Information

Transient absorption spectra observed upon 532 nm laser irradiation of **2**; potentiometric titration of **2**; quenching experiments of the triplet excited state of **3** by **4** and **5**; additional gel electrophoresis; MALDI-TOF of the construct **2**-Tel22; supplementary experimental procedures, HPLC purity data, NMR characterization of **3**. This material is available free of charge via the Internet at http://pubs.acs.org.

AUTHOR INFORMATION

Corresponding Author

Mauro Freccero mauro.freccero@unipv.it.
Sara Richter sara.richter@unipd.it

Author Contributions

‡These authors contributed equally.

Notes

The authors declare no competing financial interests.

ACKNOWLEDGMENT

This work was supported by MIUR, Grant FIRB-Ideas RBID082ATK, Grant PRIN 2009MFRKZ8 and by University of Padua and University of Pavia.

REFERENCES

1. Davis, J. T. *Angew. Chem. Int. Edit.* **2004,** *43*, 668-698.
2. Balasubramanian, S.; Hurley, L. H.; Neidle, S. *Nat. Rev. Drug Discov.* **2011,** *10*, 261-75.
3. Neidle, S. *FEBS J.* **2010,** *277*, 1118-25.
4. Biffi, G.; Tannahill, D.; McCafferty, J.; Balasubramanian, S., *Nat. Chem.* **2013,** *5*, 182-186.
5. (a) Di Antonio, M.; Doria, F.; Richter, S. N.; Bertipaglia, C.; Mella, M.; Sissi, C.; Palumbo, M.; Freccero, M. *J. Am. Chem. Soc.* **2009,** *131*, 13132-13141; (b) Doria, F.; Nadai, M.; Folini, M.; Di Antonio, M.; Germani, L.; Percivalle, C.; Sissi, C.; Zaffaroni, N.; Alcaro, S.; Artese, A.; Richter, S. N.; Freccero, M. *Org. Biomol. Chem.* **2012,** *10*, 2798-2806; (c) Nadai, M.; Doria, F.; Di Antonio, M.; Sattin, G.; Germani, L.; Percivalle, C.; Palumbo, M.; Richter, S. N.; Freccero, M. *Biochimie* **2011,** *93*, 1328-1340.
6. Doria, F.; Nadai, M.; Folini, M.; Scalabrin, M.; Germani, L.; Sattin, G.; Mella, M.; Palumbo, M.; Zaffaroni, N.; Fabris, D.; Freccero, M.; Richter, S. N. *Chem—Eur J* **2013,** *19*, 78-81.
7. Bertrand, H.; Bombard, S.; Monchaud, D.; Talbot, E.; Guedin, A.; Mergny, J. L.; Grunert, R.; Bednarski, P. J.; Teulade-Fichou, M. P. *Org. Biomol. Chem.* **2009,** *7*, 2864-71.
8. Di Antonio, M.; McLuckie, K. I.; Balasubramanian, S. *J. Am. Chem. Soc.* ***2014****, 136, 5860–5863*.
9. Percivalle, C.; Doria, F.; Freccero, M. *Curr. Org. Chem.* **2014,** *18*, 19-43.
10. Xu, Y.; Tashiro, R.; Sugiyama, H. *Nat. Protoc.* **2007,** *2*, 78-87.
11. Williamson, J. R.; Raghuraman, M. K.; Cech, T. R. *Cell* **1989,** *59*, 871-80.
12. Su, D. G.; Fang, H.; Gross, M. L.; Taylor, J. S. *Proc. Natl. Acad. Sci. U.S.A.* **2009,** *106*, 12861-6.
13. Verga, D.; Hamon, F.; Poyer, F.; Bombard, S.; Teulade-Fichou, M. P. *Angew. Chem. Int. Edit.* **2014,** *53*, 994-998.
14. Yuan, L. B.; Tian, T.; Chen, Y.; Yan, S. Y.; Xing, X. W.; Zhang, Z. A.; Zhai, Q. Q.; Xu, L.; Wang, S. O.; Weng, X. C.; Yuan, B. F.; Feng, Y. Q.; Zhou, X. *Sci Rep-Uk* **2013,** *3*.
15. (a) Schreier, W. J.; Kubon, J.; Regner, N.; Haiser, K.; Schrader, T. E.; Zinth, W.; Clivio, P.; Gilch, P. *J. Am. Chem. Soc.* **2009,** *131*, 5038; (b) Huang, Y. C.; Sen, D. *J. Am. Chem. Soc.* **2010,** *132*, 2663-2671.
16. (a) Suraru, S. L.; Zschieschang, U.; Klauk, H.; Wurthner, F. *Chem. Commun.* **2011,** *47*, 11504-11506; (b) Fin, A.; Petkova, I.; Doval, D. A.; Sakai, N.; Vauthey, E.; Matile, S. *Org. Biomol. Chem.* **2011,** *9*, 8246-8252; (c) Roger, C.; Wurthner, F. *J. Org. Chem.* **2007,** *72*, 8070-8075.
17. (a) Doria, F.; Manet, I.; Grande, V.; Monti, S.; Freccero, M., *J. Org. Chem.* **2013,** *78*, 8065-73; (b) Doria, F.; Nadai, M.; Sattin, G.; Pasotti, L.; Richter, S. N.; Freccero, M. *Org. Biomol. Chem.* **2012,** *10*, 3830-40; (c) Doria, F.; di Antonio, M.; Benotti, M.; Verga, D.; Freccero, M. *J. Org. Chem.* **2009,** *74*, 8616-25.
18. (a) Rhile, I. J.; Mayer, J. M. *Angew. Chem. Int. Edit.* **2005,** *44*, 1598-1599; (b) Thomas, F.; Jarjayes, O.; Jamet, M.; Hamman, S.; Saint-Aman, E.; Duboc, C.; Pierre, J. L. *Angew. Chem. Int. Edit.* **2004,** *43*, 594-597.
19. Rogers, J. E.; Weiss, S. J.; Kelly, L. A. *J. Am. Chem. Soc.* **2000,** *122*, 427-436.
20. Freccero, M.; Pratt, A.; Albini, A.; Long, C. *J. Am. Chem. Soc.* **1998,** *120*, 284-297.
21. Maki, T.; Araki, Y.; Ishida, Y.; Onomura, O.; Matsumura, Y. *J. Am. Chem. Soc.* **2001,** *123*, 3371-2.
22. Shaw, A. A.; Falick, A. M.; Shetlar, M. D. *Biochemistry* **1992,** *31*, 10976-10983.

TOC